

## Supplementary material

### Heterogeneous catalytic oxidation of furfural with hydrogen peroxide over a niobia catalyst

Wander Y. Perez-Sena<sup>a</sup>, Maëlle Paya<sup>a</sup>, Kari Eränen<sup>a</sup>, Robert Lassfolk<sup>b</sup>, Lucas Lagerquist<sup>c</sup>, Narendra Kumar<sup>a</sup>, Atte Aho<sup>a</sup>, Antonio D'Angelo<sup>a,d</sup>, Tapio Salmi<sup>a</sup>, Johan Wärnä<sup>a</sup>, Dmitry Yu. Murzin<sup>a</sup>

<sup>a</sup> Laboratory of Industrial Chemistry and Reaction Engineering, Johan Gadolin Process Chemistry Centre, Åbo Akademi University, FI-20500 Turku/ Åbo, Finland

<sup>b</sup> Turku Centre for Chemical and Molecular Analytics, Åbo Akademi University, FI-20500 Turku/ Åbo, Finland

<sup>c</sup> Laboratory of Organic Chemistry, Johan Gadolin Process Chemistry Centre, Åbo Akademi University, FI-20500 Turku/ Åbo, Finland

<sup>d</sup> Process and Systems Engineering Laboratory, Åbo Akademi University, FI-20500 Turku/ Åbo, Finland

#### 1) Catalyst characterization

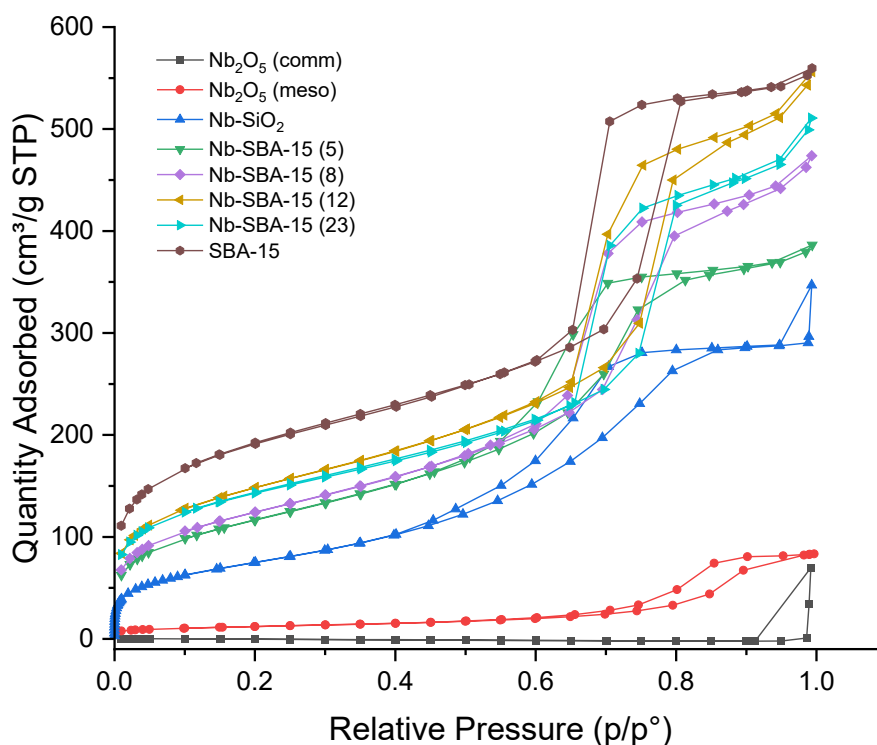


Figure S1. N<sub>2</sub> adsorption–desorption isotherms of the various niobium catalyst

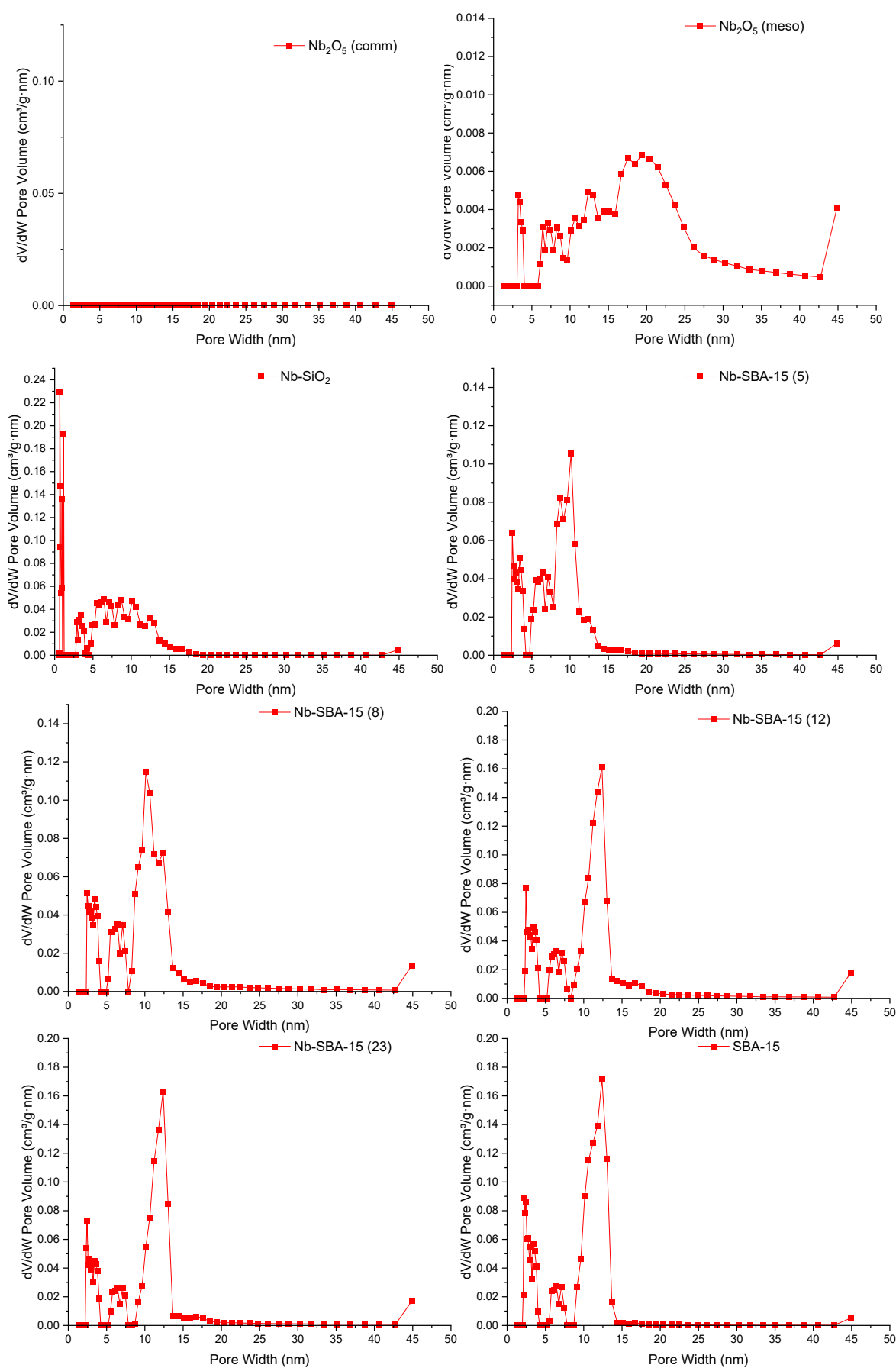


Figure S2. Pore size distributions of the various niobium catalyst calculated by NLDFT method.

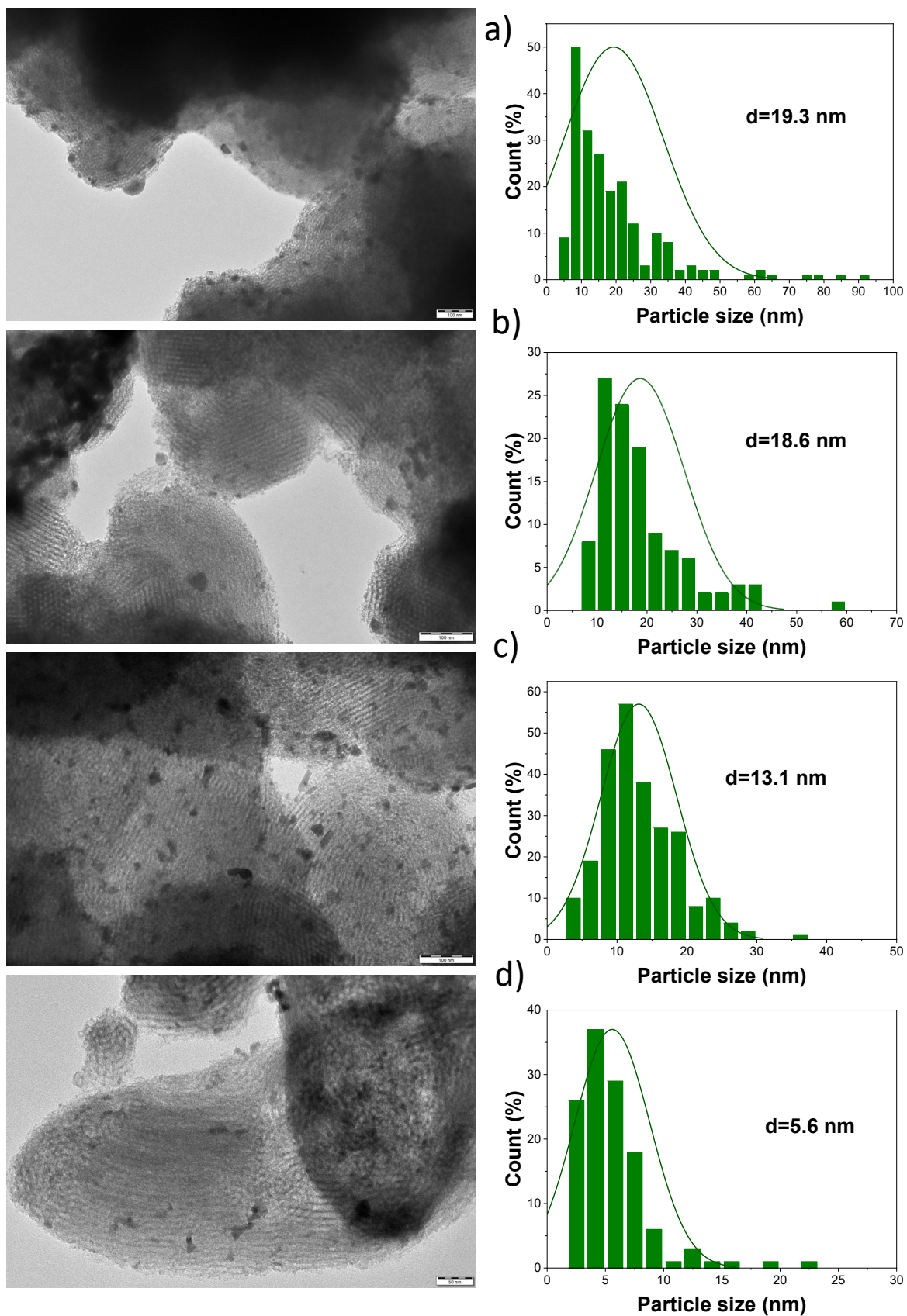


Figure S3. TEM images and particle size distribution a) Nb-SBA-15 (5), b) Nb-SBA-15 (8), c) Nb-SBA-15 (12), d) Nb-SBA-15 (23).

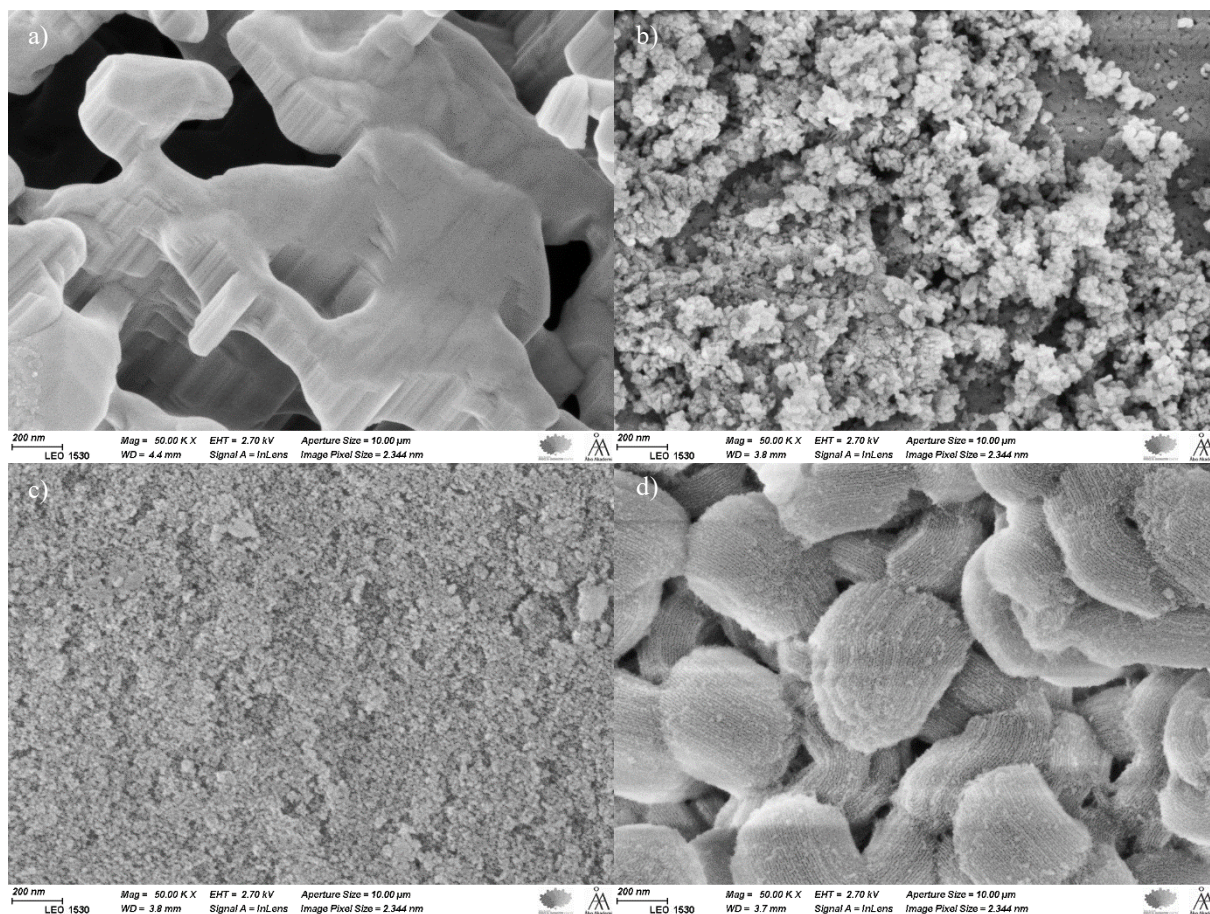


Figure S4. Scanning electron micrographs of the niobium catalysts (spacebar = 200nm):  
a) Nb<sub>2</sub>O<sub>5</sub> (comm), b) Nb<sub>2</sub>O<sub>5</sub> (meso), c) Nb-SiO<sub>2</sub>, d) Nb-SBA-15(12).

## 2) Catalyst activity and reaction products analysis

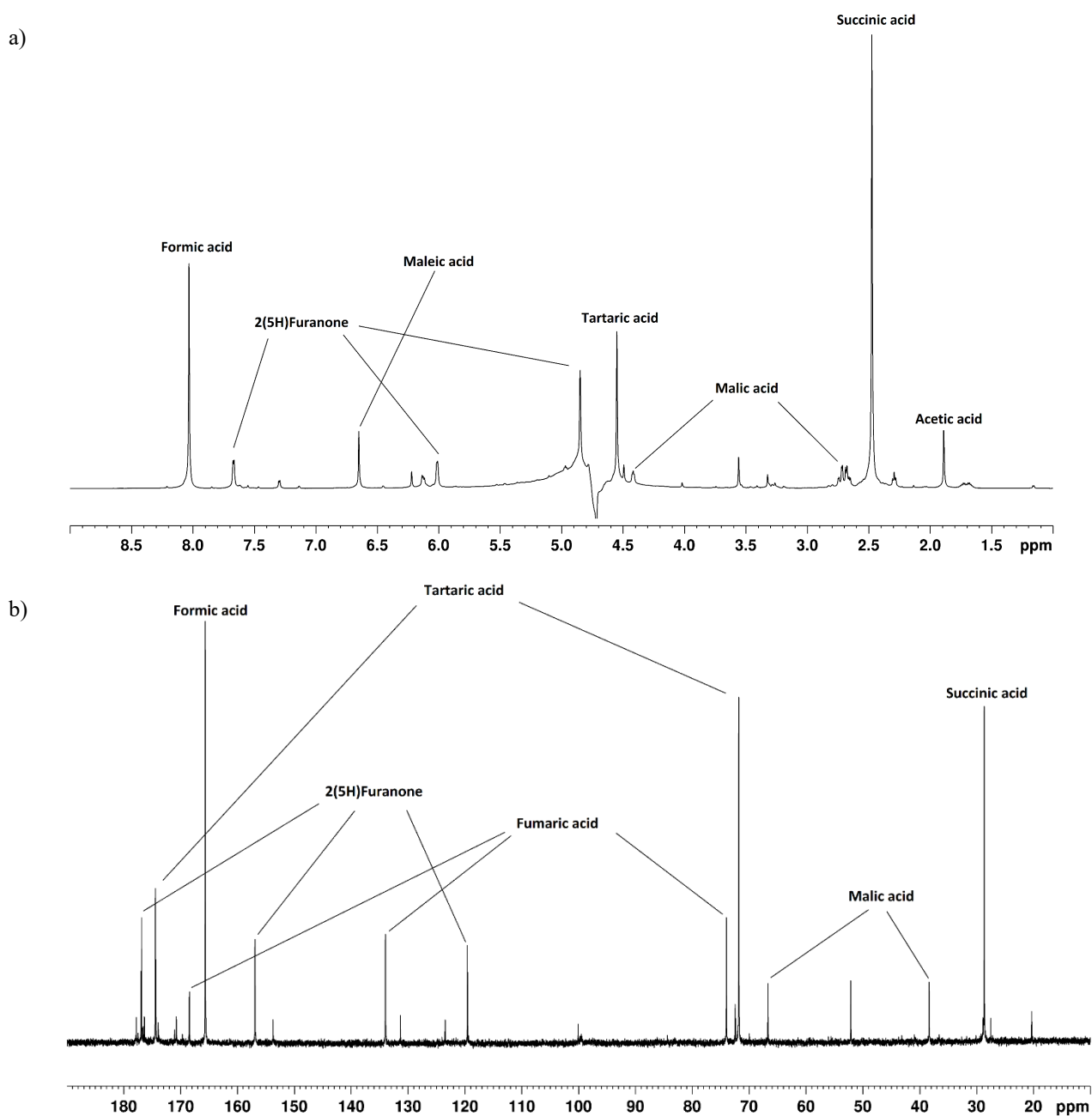


Figure S5. NMR spectra of the reaction products: a)  $^1\text{H}$  NMR, b)  $^{13}\text{C}$  NMR.

### GC-MS analysis of the reaction products

To prepare the samples for GC-MS analysis, the reaction mixture was collected after 7 hours of reaction and filtered to remove the catalyst. The resulting product mixture was freeze-dried to obtain a solid containing the oxidation products. The sample was, thereafter, subjected to a derivatization procedure to volatilize the oxidation products: approximately 1 mg of the freeze-

dried solid and 1 mL of dried pyridine were placed in a clean vial. Next, 3 drops of hexamethyldisilane and chlorotrimethylsilane were added and mixed well.

The prepared sample was injected into a gas chromatograph (Agilent Technologies, 7890A) equipped with an HP-1 (30 m × 250 μm × 0.25 μm) capillary column and a mass spectrometer (Agilent Technologies, 5975C). The GC temperature was initially set to 80 °C and then heated to 300 °C at a rate of 15 °C/min. The injection volume was 1 μL, and helium was used as the gas carrier at a flow rate of 0.9 mL/min. The temperature of the ion source was set to 230 °C for the mass selective detector. The oxidation products were identified by comparing the obtained spectra with those in the NIST Mass Spectral library.

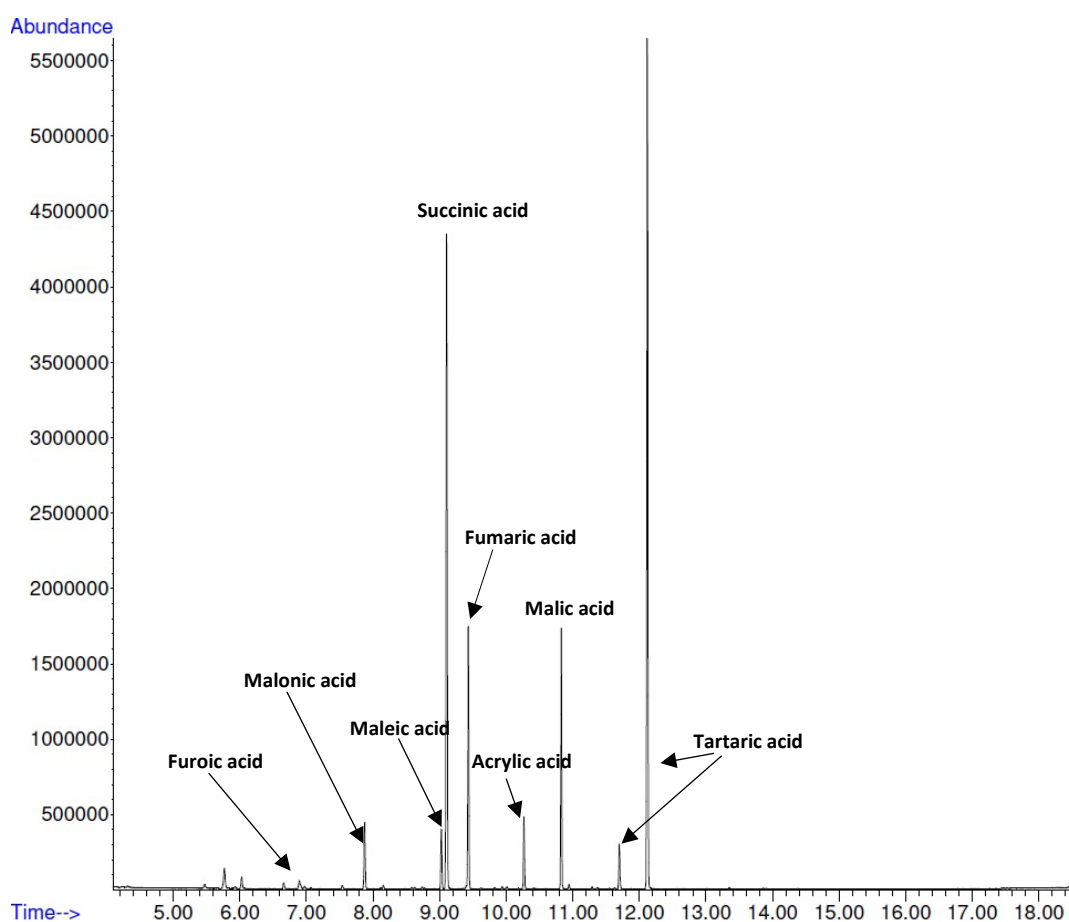


Figure S6. GC spectra of the furfural oxidation products using a niobium catalyst.

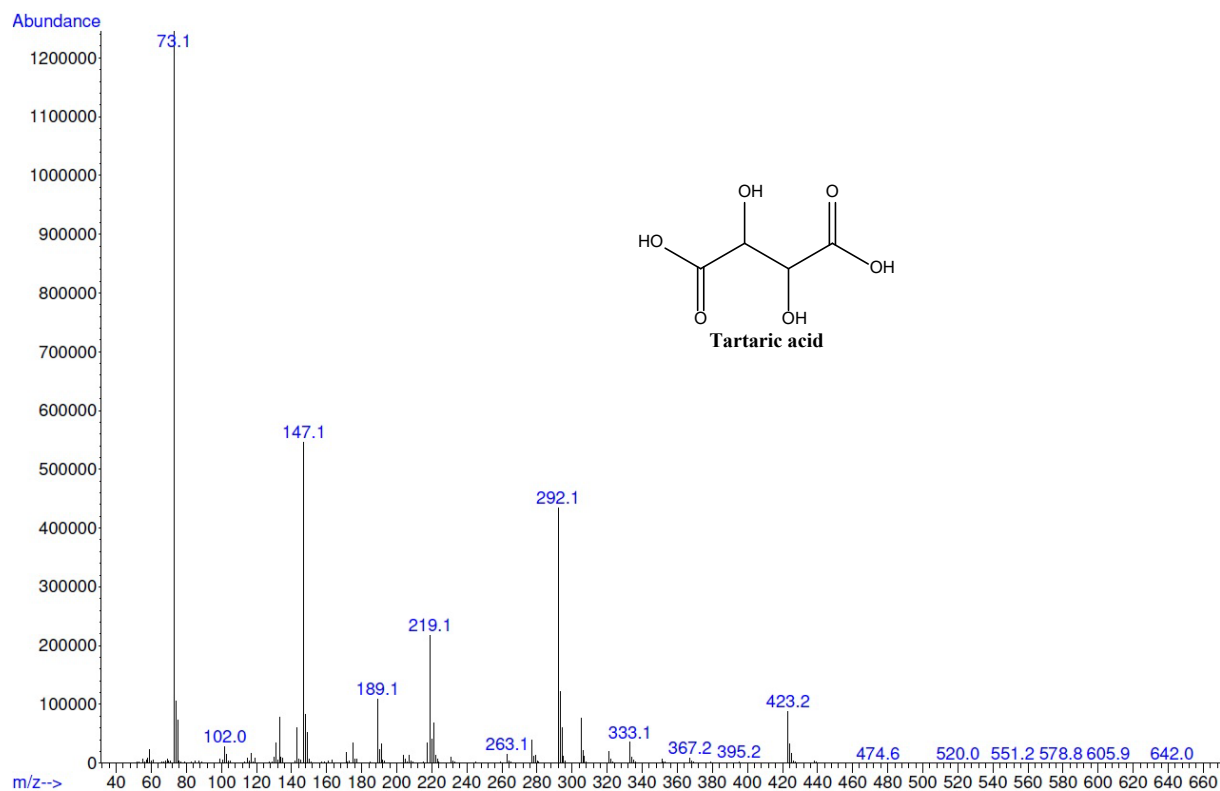


Figure S7. GC-MS spectrum of tartaric acid in the furfural oxidation products sample.

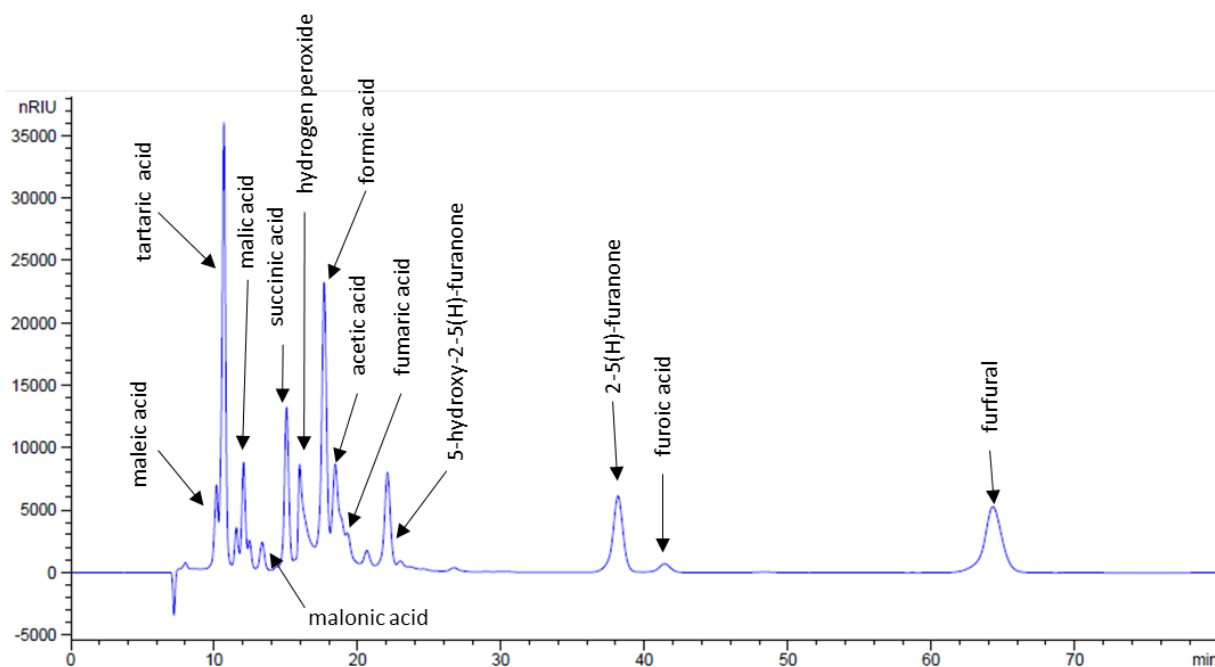


Figure S8. Typical HPLC chromatograms displaying tartaric acid and various other products during the oxidation of furfural over niobia catalyst.

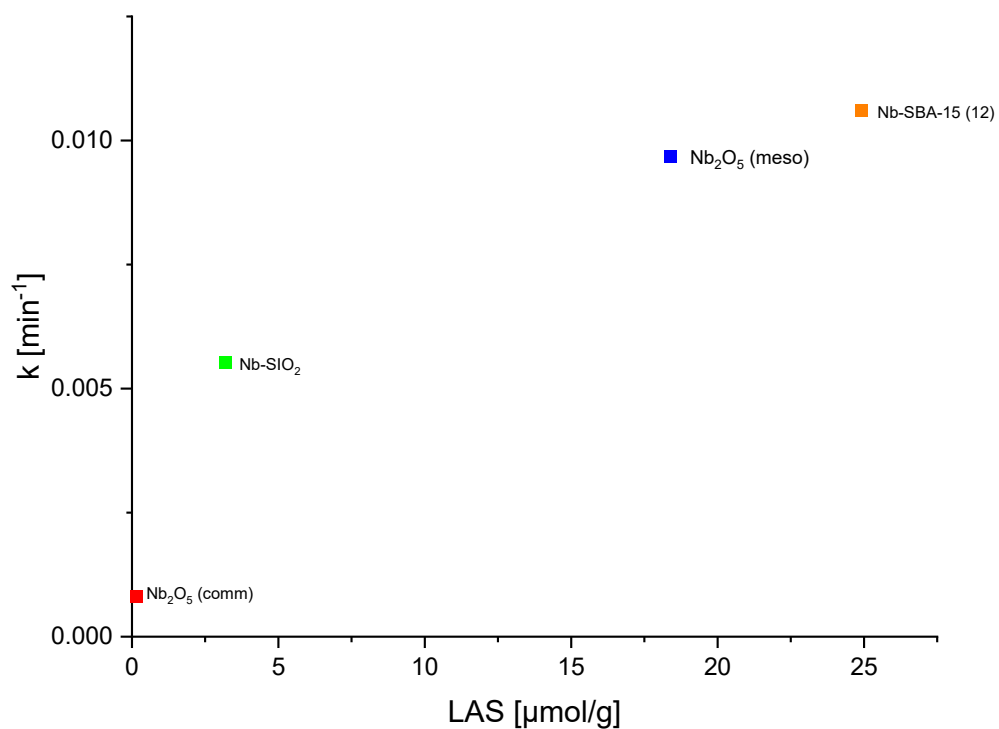


Figure S9. Rate constant of furfural oxidation and its dependency on the catalyst Lewis acidity.

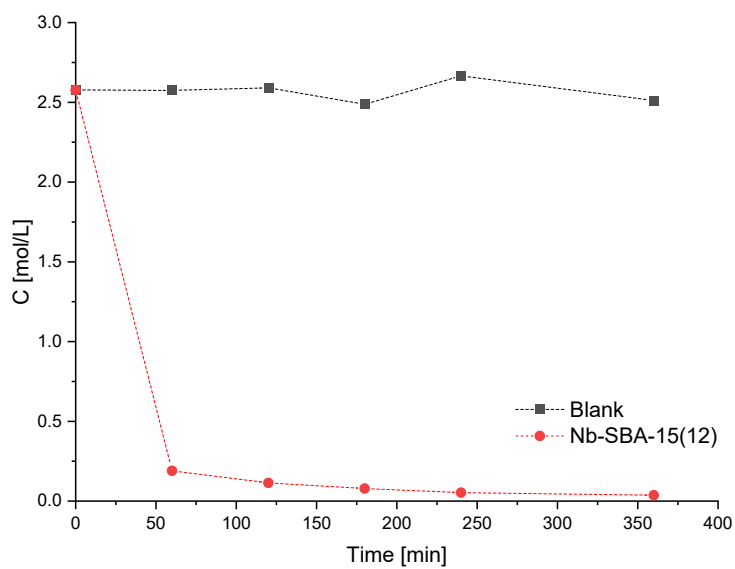


Figure S10. Hydrogen peroxide decomposition experiment. Condition;  $V_t=4$  ml, 80°C, 50mg of catalyst and 600 rpm



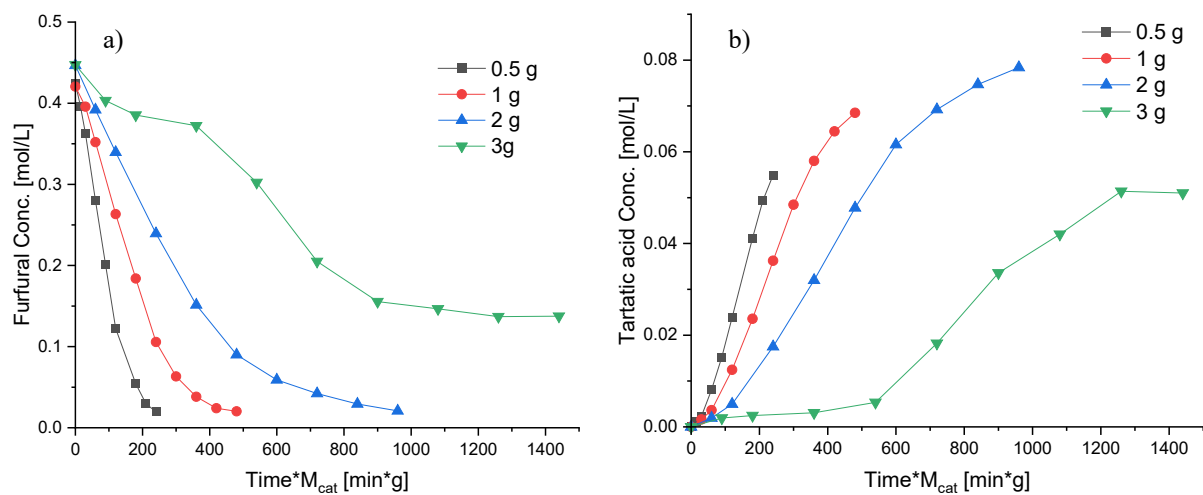


Figure S11. Catalyst loading non-proportional effect on the furfural oxidation using Nb-SBA-15 under semibatch conditions at the HP addition rate =  $4.15 \text{ ml} \cdot \text{min}^{-1}$ ,  $80^\circ\text{C}$ , Fu:HP = 1:4 and 700 rpm; a) furfural consumption b) tartaric acid formation.

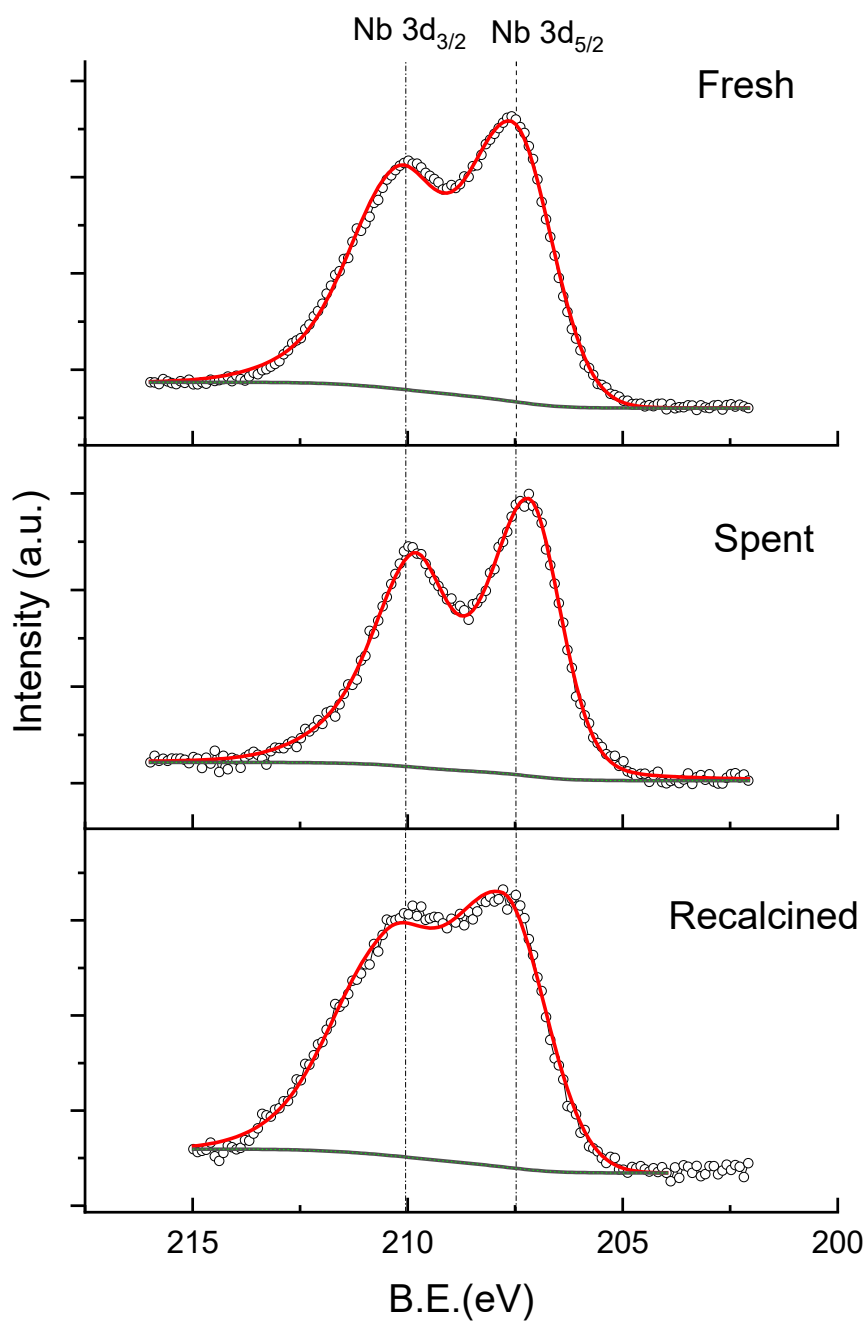


Figure S12. XPS spectra of the fresh, spent and recalcined Nb-SBA-15(12) catalyst during the stability experiments.

### 3) Reaction network elucidation

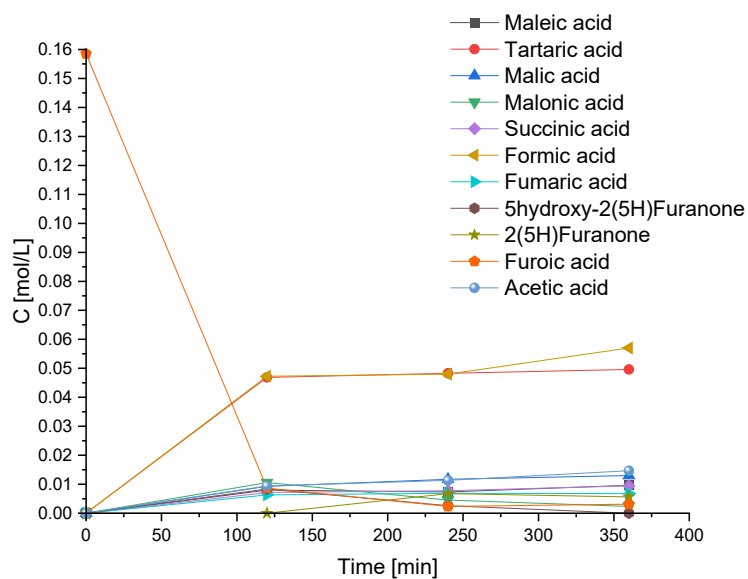


Figure S13. Oxidation of furoic acid using Nb-SBA-15. Condition;  $V_t=4.9\text{ml}$ ,  $80^\circ\text{C}$ , FuA:HP = 1:11, 50mg of catalyst and 700 rpm

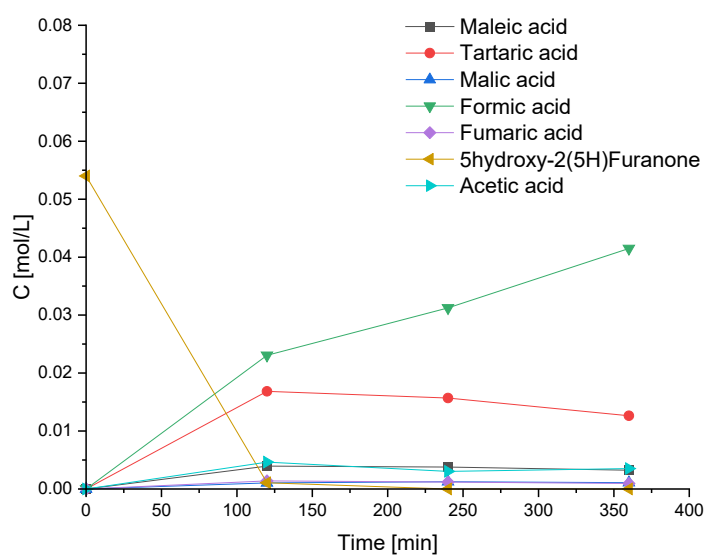


Figure S14. Oxidation of 5hydroxy-2(5H)furanone using Nb-SBA-15. Condition;  $V_t=4.9\text{ml}$ ,  $80^\circ\text{C}$ , 5hydro-2(5H)funone:HP = 1:11, 50mg of catalyst and 700 rpm

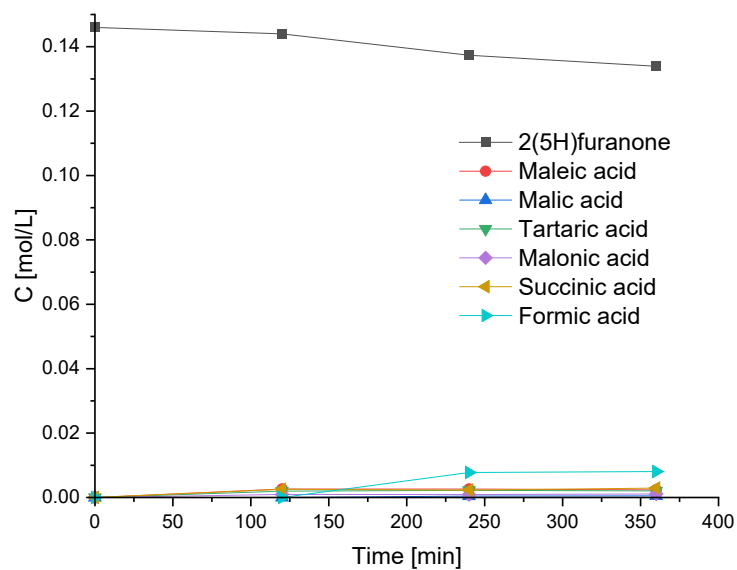
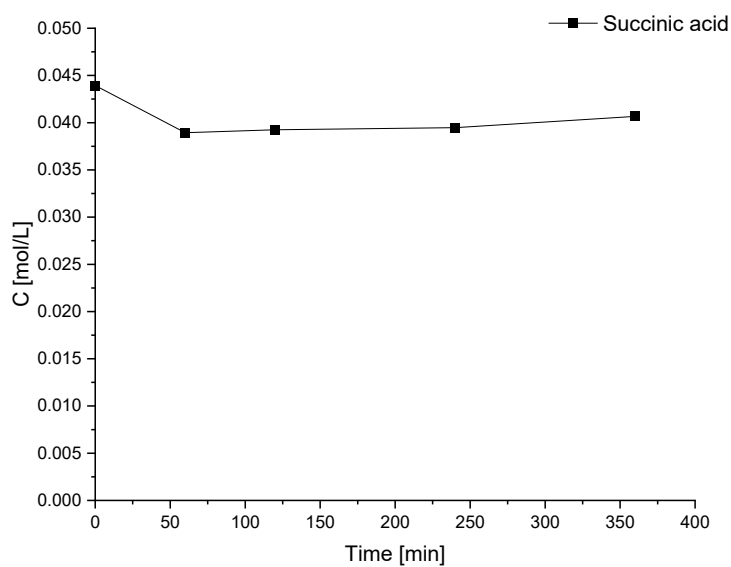


Figure S15. Oxidation of 2(5H)furanone using Nb-SBA-15. Condition;  $V_t=4.2\text{ml}$ ,  $80^\circ\text{C}$ , 2(5H)funone:HP = 1:12, 50mg of catalyst and 700 rpm



Succinic

Figure S16. Oxidation of succinic acid using Nb-SBA-15. Condition;  $V_t=4.2\text{ml}$ ,  $80^\circ\text{C}$ , SucA:HP = 1:11, 32mg of catalyst and 700 rpm

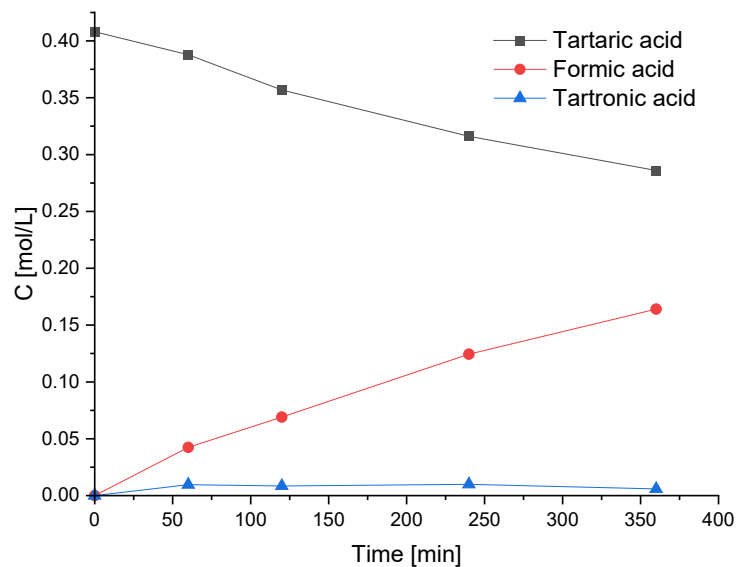


Figure S17. Oxidation of tartaric acid using Nb-SBA-15. Condition;  $V_t=4.9\text{ml}$ ,  $80^\circ\text{C}$ , TarA:HP = 1:5, 50mg of catalyst and 700 rpm

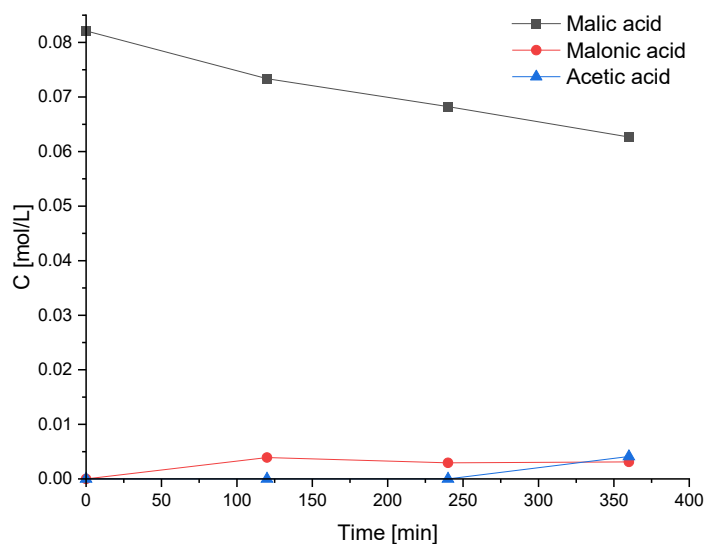


Figure S18. Oxidation of malic acid using Nb-SBA-15. Condition;  $V_t=4.9\text{ml}$ ,  $80^\circ\text{C}$ , MalA:HP = 1:11, 50mg of catalyst and 700 rpm

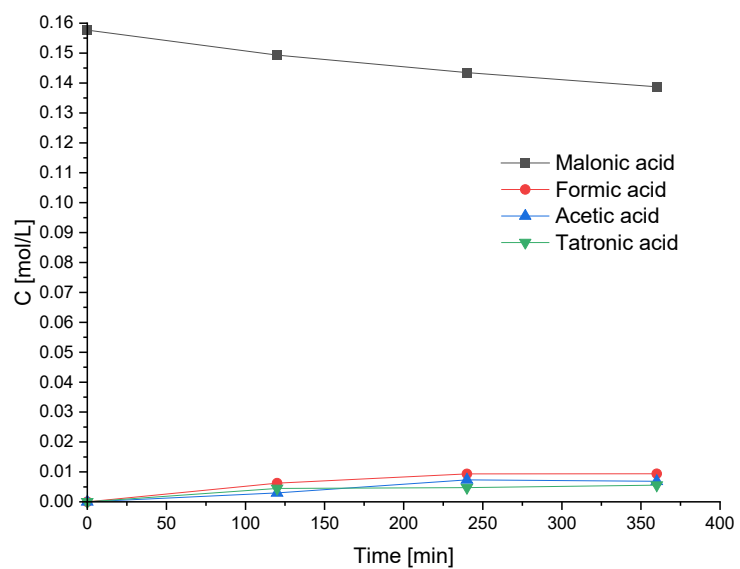


Figure S19. Oxidation of malonic acid using Nb-SBA-15. Condition;  $V_t=4.9\text{ml}$ ,  $80^\circ\text{C}$ , MaloA:HP = 1:11, 50mg of catalyst and 700 rpm